A common genetic basis to the origin of the leaf economics spectrum and metabolic scaling allometry

François Vasseur, Cyrille Violle, Brian Enquist, Christine Granier, Denis Vile

A Common Genetic Basis to the Origin of the Leaf Economics Spectrum and Metabolic Scaling Allometry

François Vasseur[1], Cyrille Violle[2,3], Brian J. Enquist[2,4], Christine Granier[1] and Denis Vile[1*]

[1]INRA, Montpellier SupAgro, UMR759 Laboratoire d'Ecophysiologie des Plantes sous Stress Environnementaux (LEPSE), F-34060 Montpellier, France

[2]Departement of Ecology and Evolutionary Biology, University of Arizona, 1041 E Lowell St., Tucson, Arizona, 85721, USA

[3]CNRS, UMR5175, Centre d'Ecologie Fonctionnelle et Evolutive, F-34000 Montpellier, France

[4]The Santa Fe Institute, 1399 Hyde Park Road, Santa Fe, New Mexico 87501, USA

*Corresponding author.

Email addresses

François Vasseur: vasseur@supagro.inra.fr; Cyrille Violle: cyrille.violle@cefe.cnrs.fr; Brian J. Enquist: benquist@email.arizona.edu; Christine Granier: christine.granier@supagro.inra.fr; Denis Vile: denis.vile@supagro.inra.fr

Author Contributions FV, CV, BJE, CG and DV designed and conceptualized the study, FV, CV, DV performed the experiments, and carried out the statistical analyses. FV, CV, BJE, CG and DV interpreted the results and wrote the paper. FV, CV and DV contributed equally to this work.

Corresponding author details:

Dr. Denis Vile

Tel.: +33499613187

Fax: +33467522116

Email: denis.vile@supagro.inra.fr

Running title: Genetics of Plant Allometry and Leaf Economics

Keywords (10): Leaf economics spectrum; metabolic scaling theory; plant allometry; quantitative trait loci; *Arabidopsis thaliana*; functional trait; net photosynthetic rate; growth rate; flowering time; life history.

Type of article: Letter.

Number of words: in the abstract (**156**), in the manuscript as a whole (**7120**), and in the main text (**5028**) (excluding abstract, acknowledgements, references, table and figure legends).

Number of references: **50**.

Number of figures and tables: 5 figures and 1 table.

Abstract

Many facets of plant form and function are reflected in general cross-taxa scaling relationships. Metabolic scaling theory (MST) and the leaf economics spectrum (LES) have each proposed unifying frameworks and organizational principles to understand the origin of botanical diversity. Here we test the evolutionary assumptions of MST and the LES using a cross of two genetic variants of *Arabidopsis thaliana*. We show that there is enough genetic variation to generate a large fraction of variation in the LES and MST scaling functions. The progeny sharing the parental, naturally occurring, allelic combinations at two pleiotropic genes exhibited the theorized optimum ¾ allometric scaling of growth rate and intermediate leaf economics. Our findings: (i) imply that a few pleiotropic genes underlie many plant functional traits and life histories; (ii) unify MST and LES within a common genetic framework; and (iii) suggest that observed intermediate size and longevity in natural populations originates from stabilizing selection to optimize physiological trade-offs.

Introduction

Since Julian Huxley (1932) showed that traits covaried with each other according to simple mathematical relationships, understanding covariation of traits within integrated phenotypes has been a central focus of comparative biology (Gould 1966; Coleman *et al.* 1994). Organismal size is a central trait in biology and influences how numerous traits and ecological processes, and dynamics covary (Niklas 1994). The dependence of a given biological trait, Y, on organismal mass, M, is known as allometry (Huxley 1932). Allometric relationships are characterized by 'power laws' where traits vary or scale with M as:

$$Y = Y_0 M^{\theta} \quad (1)$$

where θ is the scaling exponent and Y_0 is a normalization constant that may be characteristic of a given genotype or taxon. A sampling of *intra*- and *inter*-specific data reveals that the central tendency of θ often approximates quarter-powers (Niklas 1994; e.g., 1/4, 3/4, 3/8, etc.), although for any given relationship considerable variation may exist (Glazier 2005; Price *et al.* 2007) and the 'canonical' value of θ is still debated (Riisgard 1998; Kolokotrones *et al.* 2010), notably within vascular plants (Reich *et al.* 2006; Enquist *et al.* 2007b; Mori *et al.* 2010).

In addition to allometric scaling, other scaling relationships between traits have also been reported. For example, the trade-offs that govern the carbon and nutrient economy of plants appear to generate trait covariation functions that are also approximate power-laws (Reich *et al.* 1997; Westoby *et al.* 2002). Indeed, the nexus of trait correlations that makes up the leaf economics spectrum (LES) reflects the fundamental trade-off between the rate of acquisition of resources and lifespan (Charnov 1993; Reich *et al.* 1997; Wright *et al.* 2004; Shipley *et al.* 2006; Blonder *et al.* 2011). The LES describes how multiple physiological and morphological leaf traits, including net photosynthetic rate, dry mass per area (LMA), longevity, and nitrogen (N) concentration, covary across vascular plant taxa. This spectrum of covariations reflects the fact that leaves with long lifespan require more structural investment

78 (associated with high LMA, reduced CO_2 permeability and light intensity inside the leaf), and
79 a low mass-based photosynthetic and respiration rate (Kikuzawa 1991; Reich *et al.* 1997;
80 Wright *et al.* 2004; Blonder *et al.* 2011). Conversely, high rates of photosynthesis are
81 characterized by low LMA values. Further, low LMA leaves are more vulnerable to herbivory
82 and physical damages (Kikuzawa 1991; Westoby *et al.* 2002). The LES appears to be
83 universal across biomes and has been applied to understand functional variation in scaling
84 relationships at whole-plant (Baraloto *et al.* 2010) and community (Kikuzawa & Lechowicz
85 2006) levels.

86 Metabolic scaling theory (MST) posits that various scaling exponents in biology – most
87 notably, the scaling of whole plant metabolism (B) and growth rate (dM/dt) with M – are the
88 result of natural selection on the scaling of whole-plant resource use. In particular, MST
89 hypothesizes that for volume-filling vascular networks, natural selection will act to maximize
90 the scaling of whole-organism resource uptake but simultaneously minimize the scaling of
91 vascular transport resistance (West *et al.* 1999a). As a result, values of θ will tend to cluster
92 around 'quarter-powers' so that $dM/dt \propto B \propto M^{3/4}$. However, in making this assumption, MST
93 implicitly assumes that there is potential variation in θ and that this variation is heritable
94 (Enquist & Bentley 2012). Indeed, elaborations of MST openly state that selection is expected
95 to act on θ (Price *et al.* 2007; Olson *et al.* 2009) but we know of no examples showing a clear
96 genetic basis to the scaling exponents highlighted by MST.

97 Similarly to MST, explanations for the LES are framed in the context of how selection
98 optimizes the trade-off between investment for organ longevity and return on investment in
99 carbon and nitrogen (Kikuzawa 1991; Westoby *et al.* 2000). Because of the physiological
100 linkages between the traits that govern leaf economics, the global variation of many of the
101 LES traits have been hypothesized to be under the control of a common genetic mechanism
102 (Chapin *et al.* 1993). Consistent with this hypothesis, several pleiotropic genes underlying

many continuous traits related to plant development, physiology and growth have been identified in Arabidopsis (e.g. McKay *et al.* 2003; Masle *et al.* 2005; Fu *et al.* 2009; Mendez-Vigo *et al.* 2010) and other species (e.g. Poorter *et al.* 2005; Edwards *et al.* 2011). The evolutionary importance of pleiotropic genes in explaining observed coordinated changes in covarying traits has been intensively debated (e.g. Pavlicev & Wagner 2012). Because of the difficulty of measuring traits related to carbon fixation (but see Edwards *et al.* 2011; Flood *et al.* 2011), the genetic bases underlying plant life histories and the LES remained to be elucidated. Thus, the role of pleiotropic genes and genetic constraints in shaping the evolutionary dynamics of plant functional diversity is unclear (Donovan *et al.* 2011).

Arguments for the origin of the scaling relationships described by the LES and MST have not been tested. In particular, they make two implicit evolutionary assumptions. First, they assume that there is variation in the subsidiary traits underpinning scaling relationships. Secondly, they assume that subsequent Darwinian selection on scaling relationships occurs at the *intra*-specific level. However, studies that have assessed the predictions and generality of the LES and MST have mainly been conducted at the *inter*-specific level. Here, we test the evolutionary assumptions of botanical scaling theory. We characterized the scaling of carbon and nutrient economics and the allometric scaling of growth rate across numerous Arabidopsis genotypes spanning 3 orders of magnitude in size.

We utilized a powerful high-throughput phenotyping platform (Granier *et al.* 2006) to grow a population of recombinant inbred lines or RILs under strictly controlled environmental conditions. Two pleiotropic quantitative trait loci (QTL) with major effects (*EDI* and *FLG*) have been identified through the analysis of plant development and life history in these RILs (Alonso-Blanco *et al.* 1998b; El-Assal *et al.* 2001; Doyle *et al.* 2005; Fu *et al.* 2009). Allelic variability in these genes leads to a corresponding diversity in the timing of flowering, the rate of leaf production and the general pattern of vegetative growth (Mendez-Vigo *et al.* 2010).

We hypothesize that variation in life history, in particular the time to reach reproductive maturity, has important consequences for the lifetime carbon and nutrient budget at the leaf and whole-plant levels. As a result, selection should act on the scaling of carbon and nutrient budgets via the traits that underlie their physiological rates and life histories.

Material and methods

Plant material

We analyzed genetic variability in leaf economics and the scaling of plant growth across the RILs previously generated from a cross between Landsberg *erecta* (L*er*) and Cape Verde Islands (Cvi) (Alonso-Blanco *et al.* 1998a), two accessions that derived from contrasted locations. We also selected near isogenic lines (NILs) and targeted mutants to confirm the quantitative trait loci (QTL) identified from the genetic analysis and test candidate genes, respectively. NILs were chosen from the population previously developed by introgressing genomic regions Cvi into L*er* (Keurentjes *et al.* 2007). The NIL LCN 1-2.5 (NASC code N717045; Cvi-EDI_{Ler}) carries a Cvi fragment at the top of chromosome I and was selected to confirm the *EDI* locus. LCN 5-7 (N717123; Cvi-FLG_{Ler}) carries a Cvi fragment in the middle of chromosome V and was selected to confirm the *FLG* locus. Genetic and molecular studies have identified two candidate genes of the regulatory pathway of circadian clock as major contributors of *EDI* and *FLG* effects: *CRY2*, a gene coding a blue-light receptor (El-Assal *et al.* 2001), and *HUA2*, a gene coding a transcription factor of the AGAMOUS pathway (Doyle *et al.* 2005), respectively. We selected two knock-out mutants to investigate the candidate gene *CRY2*: one in Col-4 background (N3732; $cry2_{Col}$) and one in L*er* background (N108; $cry2_{Ler}$). To investigate the candidate gene *HUA2*, we selected a knock-out mutant of *HUA2* in Col-0 (N656341; $hua2_{Col}$). The choice of Col background was motivated by the collection of mutants available in stock centers.

153

154 ## *Growth conditions*

155 We performed two experiments utilizing the PHENOPSIS automated growth chamber
156 (Granier *et al.* 2006). The PHENOPSIS facility maintains constant growing environment and
157 allows for the precise temporal monitoring and automated measurements of 504 potted plants.
158 In Experiment 1, we phenotyped the parental accessions (L*er* and Cvi; $n = 8$ replicates) and
159 120 RILs ($n = 4$) selected from the 162 available lines (See Appendix S1 in Supporting
160 Information). Plants were grown in four randomized blocks. In Experiment 2, we phenotyped
161 the two parental accessions ($n = 8$), 16 RILs ($n = 6$) spanning the range of trait variability
162 observed in Experiment 1, the NILs ($n = 7$), and the mutants and associated wild-types (both n
163 = 10). All detailed growing and meteorological conditions are given in Appendix S1 and
164 Table S1 therein, in Supporting Information.

165

166 ## *Measurements of plant traits*

167 The total projected leaf area of the rosette (RA, cm^2) was determined every 2 to 3 days
168 from zenithal images of the plants. A sigmoid curve was fitted for each plant following:

169 $$RA = \frac{a}{1+e^{\left(\frac{(d-d_0)}{b}\right)}} \quad (1)$$

170 where d is the number of days after emergence of the firsts two true leaves, a is the maximum
171 vegetative rosette area, d_0 is the time when $a/2$ leaf area has expanded and b is related to the
172 maximum rate of leaf production. The maximum rate of leaf expansion (R_{max}, $m^2\ d^{-1}$) was
173 calculated from the first derivative of the logistic model at d_0 as $R_{max} = a/(4b)$.

174 Photosynthesis was measured at flowering and under growing conditions using a whole-
175 plant chamber prototype designed for Arabidopsis by M. Dauzat (INRA, Montpellier, France)
176 and K.J. Parkinson (PP System, UK) and connected to an infrared gas analyzer system

177 (CIRAS 2, PP systems, USA). To insure plant gas exchange was not corrupted by soil
178 respiration, we sealed the soil surface with four layers of plastic film. The flowering stem was
179 detached from the rosette before measurement to record leaf gas exchange only. Whole-plant
180 photosynthetic rate was expressed on a dry mass basis (nmol g^{-1} s^{-1}).
181 All plants were harvested after photosynthetic measurements. Each rosette was cut,
182 wrapped in moist paper and kept at 4 °C overnight in darkness to achieve complete
183 rehydration. Leaf blades were then separated from their petiole and scanned for area
184 measurements. Next, both were oven-dried at 65 °C for 72 h and their dry weight was
185 determined. Aboveground plant dry mass (*M*, mg) was determined as the sum of dry mass of
186 petioles and blades. Total leaf area (cm^2) was determined as the sum of individual leaf blade
187 areas. Leaf dry mass per area (LMA, g m^{-2}) was calculated as the ratio of dry mass and total
188 leaf area. Assuming that LMA did not vary over time during the period of maximum
189 expansion rate, we calculated maximum absolute growth rate (*G*, g dry mass d^{-1}) from R_{max}
190 and LMA. In order to obtain sufficient dried material for chemical analyses, leaf blades and
191 petioles were ground together to determine N concentration by mass spectrometry (EA2000,
192 Eurovec, Isoprime, Elementar). Leaf lifespan was estimated from the oldest active leaf that
193 showed some signs of senescence at harvest from the daily pictures of the 16 RILs in
194 Experiment 2. This estimation was used to test the relationship between age at flowering and
195 leaf lifespan (See Appendix S2). Traits were measured on each individual, except N
196 concentration which was measured on a single replicate in Experiment 1 and on three
197 replicates in Experiment 2. Phenotypic data are stored in the PHENOPSIS database (see
198 Appendix S1).
199

Statistical analyses

We first assessed the allometric relationship between aboveground dry mass (M) and maximum absolute growth rate (G) across all RILs by fitting a linear model: $\log_{10}(G) = \log_{10}(b_0) + b_1\log_{10}(M)$. Inspection of the residuals from this model revealed a significant departure from linearity (Figs S1 and S2). Next, following Kolokotrones *et al.* (2010), we fit a nonlinear quadratic model: $\log_{10}(G) = \log_{10}(b_0) + b_1\log_{10}(M) + b_2(\log_{10}(M))^2$, using the Generalized Estimation Equation (*gee* package in the statistical program R 2.12). The slope θ_q of the quadratic at any given M value was calculated as the derivative of the quadratic function $\theta_q = b_1 + 2b_2\log_{10}(M)$.

Broad-sense heritability (H^2) of each trait was estimated as the ratio of (among – within) lines (RILs) to total (among + within) variance components with replicate plant within RIL treated as random effect (R/*nlme* package).

We used 144 AFLP markers spanning all the genome to perform a QTL analysis of all traits by composite interval mapping (R/*qtl* package). For each trait, 5%-level significance threshold for QTL LOD scores were calculated following 1000 permutations. Here, this threshold did not exceed 2.9. Relationship QTLs (rQTLs) were detected by testing the allelic effect on the major axis slope of the allometric relationship at each locus (Tisné *et al.* 2008; Pavlicev & Wagner 2012; Fig. S3).

Results

Across the RILs, we observed a considerable amount of trait variation. All of the morphological, physiological and growth-related traits showed significant between-line variance ($P < 0.001$) despite the weak differences between the parental accessions L*er* and Cvi (Fig. 1 and Table S2). Interestingly, the range of variation in these traits was often a considerable fraction of the global variation in these traits (see Fig. S4). Broad sense heritabilities ranged from 0.68 (LMA) to 0.89 (plant dry mass) (Table 1). Such high heritability values reflect the important role of genetics in determining the observed trait variation, and also point to the low environmental variability within the PHENOPSIS automaton (e.g. lack of significant block effect for all traits (all $P > 0.10$)).

Our results show that, in accordance with MST predictions, the maximum absolute plant growth rate (G), across all RILs, scaled to the ¾-power of plant dry mass (M) (Fig. 2; $G = 6.32M^{0.76}$; $R^2 = 0.96$). However, a quadratic model better fitted to the allometric relationship so that as plant mass increases, there is a progressive shallowing of the allometric exponent, θ (Figs S1 and S2). However, as we show below, this curvilinearity was generated by a shift in scaling exponent across RILs.

Next, we determined if there was a genetic basis to the observed variation in allometric scaling. We performed a QTL detection for the allometric growth exponent, θ_q, estimated for each RIL by fitting the quadratic model, and a rQTL analysis of the relationship scaling. These two analyses identified two loci that control variation in the allometric exponent (LOD score > 2.9; Figs 3A and S3) and exhibit additive effects. These loci were: *EDI*, located at the top of chromosome 1 (CI = [5; 11] cM), and *FLG* in the middle of chromosome 5 (CI = [37; 45] cM). Their additive effect explained 68% of the total variability in θ_q (Table 1; Fig 3A and Fig. S5). As previously found through the dissection of Arabidospis' life history (Alonso-Blanco *et al.* 1998b; Mendez-Vigo *et al.* 2010), these two QTLs were also the major

244 determinants of age at flowering (Fig. 3B), indicating that variation in θ_q is also associated
245 with life history variation. We found that the subsets of RILs carrying the parental
246 combinations at *EDI* /*FLG* loci (parental types; i.e. L*er*/L*er* and Cvi/Cvi) shared a *common*
247 allometric slope ($P = 0.34$) that did not differ significantly from ¾ ($\theta = 0.77$; CI = [0.74; 0.80];
248 Fig. 2). However, the recombinant types at *EDI* /*FLG* loci displayed either significantly
249 higher (Cvi/L*er*; $\theta = 0.89$; CI = [0.85; 0.94]) or significantly lower (L*er*/Cvi; $\theta = 0.61$; CI =
250 [0.58; 0.65]) scaling exponents (both $P < 0.001$; Fig. 2). Our analysis revealed no epistatic
251 interactions between *EDI* and *FLG* ($P > 0.05$ except for N concentration, see Fig. S5).
252 A strong pattern of covariation was found across RILs between the physiological and
253 morphological traits involved in the leaf economics spectrum, LES. We found that mass-
254 based net photosynthetic rate and N concentration were positively correlated, whereas they
255 were negatively correlated with age at flowering and LMA (Table 1; Fig. 4). Our genetic
256 analysis revealed that *EDI* and *FLG* are also major pleiotropic QTLs with additive effects that
257 explained 63%, 56%, 60% and 35% of the variability in age at flowering, LMA, mass-based
258 photosynthetic rate and N concentration, respectively (Table 1; Figs 3B and S5). As a result,
259 we observed strong correlations between these traits and the allometric exponent, θ_q (Table 1).
260 Values of θ_q were positively correlated with variation in traits related to carbon fixation
261 (photosynthetic rate and N concentration) and negatively correlated with the traits related to
262 organ longevity (age at flowering and LMA). Together these results demonstrate that differing
263 allelic combinations at the *EDI* and *FLG* loci result in plants displaying significant differences
264 in leaf economics (Figs 4 and S6) with concomitantly significant changes in metabolic
265 exponent (Figs 2 and 4). Nonetheless, each of the parental types did not exhibit significant
266 changes in θ_q and each was characterized by the predicted 'optimal' ¾-power allometric
267 scaling of growth rate and intermediate LES strategies. In contrast, recombinant types showed
268 extreme LES and MST phenotypes characterized by either strongly hastened or delayed

flowering life histories. These extremes in life history are characterized by either increased or decreased LES traits and steeper or shallower allometric exponents, respectively (Fig. 2).

The role of *EDI* and *FLG* in controlling the allometric scaling of plant growth and the traits that underlie leaf economics was confirmed in Experiment 2. A high reproducibility of the phenotypes was observed among the 16 RILs grown in both experiments (correlations between trait values $r_{Spearman} > 0.93$ and $P < 0.001$). Across these 16 RILs, we observed significant differences in LES traits (Fig. S7) and allometric slopes (Fig. S8) according to the allelic combination at *EDI* and *FLG* loci. Although the values of the exponent θ_q varied from 1.33 to 0.57, the values of the parental types were again not significantly different from 0.75 ($P > 0.35$ in both parental types; Fig. S8), as observed in Experiment 1. Moreover, the introgressions of the Cvi chromosomal region carrying *EDI* or *FLG* into L*er* significantly hastened (Cvi-EDI_{Ler}) or delayed flowering (Cvi-FLG_{Ler}), respectively (Fig. 5 and Table S2), with an associated decreased or increased plant size, growth rate, LMA, photosynthetic rate and *N* concentration in a coordinated way (Fig. 5 and Table S2). For the 16 RILs grown in Experiment 2, we found a highly significant relationship between the lifespan of the oldest senescing leaf and age at flowering ($R^2 = 0.86$; $P < 0.001$; Fig. S9) indicating that at least in this population, age at flowering is a reasonable proxy for mean lifespan of the first leaves.

Lastly, we investigated the candidate genes, *CRY2* and *HUA2* as major contributors of *EDI* and *FLG* effects, respectively. The $hua2_{Col}$ KO-mutant displayed significant changes in leaf economics ($P < 0.05$ for all traits; Table S2 and Fig. 5), whereas the *CRY2* ($cry2_{Ler}$ and $cry2_{Col}$) KO-mutants displayed strong differences in age at flowering and less difference in photosynthetic rate, LMA and N concentration (Table S2 and Fig. 5). We found no difference in the phenotypes of $cry2_{Ler}$ and $cry2_{Col}$, suggesting that the genetic background did not influence our results. Finally, the effects of *CRY2* and *HUA2* on growth strategy were

confirmed since NILs and mutants displayed significant changes in plant mass but no changes in growth rate, indicating a departure from the allometric relationship.

Discussion

In this paper we assessed several of the implicit assumptions of MST and the LES. We demonstrated that a few genes can generate a large fraction of variation in MST exponents and LES traits. Within Arabidopsis, these genes appear to be responsible for constraining the covariation of the leaf economics and the allometric scaling of plant growth. Based on our findings we propose a novel conceptual framework that links the principles of MST to the LES.

Our findings support two central evolutionary assumptions of MST. First, MST implicitly assumes that selection can act on metabolic scaling exponents. In other words, there is genetic variation in metabolic scaling that selection can act upon. Interestingly, as previously observed for *inter*-specific metabolic allometric scaling of mammals (Kolokotrones *et al.* 2010) and plants (Enquist *et al.* 2007b; Mori *et al.* 2010) the relationship between whole-plant growth rate and plant biomass across RILs was curvilinear and not a pure power-law. This decrease in allometric exponent within increased size is also consistent with the decline in relative growth rate or RGR with size observed in other species (Poorter *et al.* 2005; although these RGR studies have not typically controlled for allometric effects on RGR). Importantly, our results also show that the observed allometric curvilinearity was primarily due to a mixing of different exponents across genotypes. In other words, genetic variation for the metabolic growth exponent resulted in a curvilinear 'inter-RIL' scaling allometry. Second, the subsets of inbred lines carrying the parental (naturally occurring) allelic combinations at two specific QTLs shared a *common* allometric exponent centered on

¾, whereas the recombinant types displayed higher and lower scaling exponents than the canonical '¾' hypothesized by MST (Fig. 2). These findings are consistent with a core MST assumption that 'quarter-power' scaling is the outcome of stabilizing selection on metabolic allometries (Enquist *et al.* 2007a). Interestingly, recombinant types were characterized by strongly hastened or delayed flowering, as well as increased or decreased photosynthetic rates, LMA, and N concentration, respectively (Fig. 4 and Fig. S5). Together, these findings suggest a tight coupling between life history, LES traits, and MST.

As stated by Wright *et al.* (2004), "*leaf lifespan describes the average duration of the revenue stream from each leaf constructed*". However, whole-plant growth rates and competitive ability depend not only on the photosynthetic rate of individual leaves, but also on the geometry and dynamics of a plant's canopy, and the pattern of energy allocation among all organs (Givnish 1988). We argue that, at least for annual plants in which all the leaves die almost simultaneously during the final stage of reproduction, whole-plant functioning should be tightly coupled to the lifespan of the plant (Charnov 1993). Indeed, a strong correlation between plant age at flowering and leaf longevity was found in this study and in the literature (Appendix S2 and Fig. S9). Although the comparison with the interspecific GLOPNET data (Wright *et al.* 2004) is limited due to the differences in the levels of measurement – leaf versus whole-plant level in this study –, the ratio of interquartile range for photosynthesis and LMA showed that our data span 70% and 55% of the variation in these traits, respectively (Fig. S4). In addition, the observed variation in the scaling exponents of growth rate within the RILs captures most of the variation in allometric exponents observed worldwide (Price *et al.* 2007). Measurements of plant growth and photosynthetic rate at the canopy level integrate the changes in architectural constrains associated with size, such as leaf shape and leaf overlapping. Hence, these measurements reflect the physiological trade-offs and the variation in leaf morphology such as LMA,

343 occurring at the whole-plant level. In this view, we argue that the changes in rosette
344 architecture are likely also associated with the nexus of traits and allometric covariation that
345 we observed. In particular, departure from space-filling branching for light interception, is
346 likely the reason why we observe departure from the 'allometrically ideal' MST ¾-power
347 scaling of plant growth (Price *et al.* 2007).
348
349 The effects of the QTLs responsible for the variation in the scaling relationships were
350 confirmed in the targeted NILs for which a coordinated change in the traits related to the leaf
351 economics was observed (Fig. 5 and Table S2). In most relationships we find that the parental
352 accession L*er* was closer to the parental accession Cvi (intermediate positions) than to the
353 NILs (extreme positions). This is probably due to the opposite and counterbalancing effects of
354 *EDI* (e.g. Cvi allele decreases size and age at flowering whereas it increases photosynthetic
355 rate and N concentration) and *FLG* (e.g. Cvi allele increases size and age at flowering
356 whereas it decreases photosynthetic rate and N concentration). Two genes, *CRY2* and *HUA2*
357 have been shown to be the major contributors of *EDI* and *FLG* pleiotropic effects,
358 respectively (Fu *et al.* 2009). Our results show that a single amino acid Val-to-Met
359 replacement in the Cvi allele of *CRY2* and a premature codon stop in the L*er* allele of *HUA2*
360 cause a cascade of large changes across numerous leaf physiological traits, and in the scaling
361 of plant metabolism. This shift in metabolic scaling associated with the effects of *HUA2* is
362 consistent with the change in the rate of leaf production reported by Mendez-Vigo *et al.*
363 (2010). The Cvi ecotype carries a rare allele of *CRY2*, unique over more than 100 sequenced
364 ecotypes (El-Assal *et al.* 2001), whereas the L*er* allele of *HUA2* is identified as common only
365 in ecotypes from UK and Central Europe (Doyle *et al.* 2005; Wang *et al.* 2007). Moreover,
366 Cvi is an unusual accession from the Cape Verde Islands which exhibit peculiar climatic
367 conditions. Although contrasted phenotypes could be expected in the Cvi accession, we

368 observed ‘allometric ideal’ ¾ exponent, intermediate timing of flowering and intermediate
369 leaf economics in both parental types, despite the climatic differences in the parental sites of
370 origin. We argue that these findings are in accordance with Metcalf and Mitchell-Olds (2009)
371 who hypothesized that selection to optimize the size at reproduction without sacrificing leaf
372 and whole-plant functioning has likely resulted in an intermediate timing of reproduction.
373 This explanation does not necessarily imply that flowering time is the target of natural
374 selection but rather that there are integrated physiological trade-offs linking life history, leaf
375 economics and plant allometry.

376 Our results also appear consistent with predictions from the ‘Selection, Pleiotropy and
377 Compensation’ (SPC) model of Pavlicev and Wagner (2012). Specifically, this Dobzhansky-
378 Muller view of evolutionary dynamics states that within isolated or semi-isolated populations
379 differing allelic associations of pleiotropic genes with major effects on life history and
380 physiology underlie trait covariation patterns and are possibly responsible for deleterious
381 changes in metabolic scaling. In artificially-generated RILs, the allelic association of a few
382 genes with major effects often leads to remarkably extreme phenotypes. However, these
383 extreme phenotypes likely would not be successful in nature compared to naturally occurring
384 genotypes due to hybrid breakdown (Bomblies *et al.* 2007). Specifically, the observed ¾
385 scaling exponent could be then maintained by selection because crosses between populations
386 create hybrid breakdown. Nonetheless, despite the strong genetic effect depicted by the high
387 heritabilities observed here, we strongly suggest that future tests of the evolutionary role of
388 pleiotropy in maintaining allometric scaling and life history trade-offs utilize transplant
389 experiments in the field. The massive collection of Arabidopsis accessions that are currently
390 genotyped or sequenced (e.g. Hancock *et al.* 2011) offer a promising tool to further explore
391 the genetic diversity, and elucidate the evolutionary and ecological links between variation in
392 climate and the traits that define leaf economics and metabolic allometry.

Genetic constraints, which occur when the genes controlling many correlated traits have antagonist effects, have also been proposed to shape the LES by restricting the genetic variation for each trait combination (Reich *et al.* 1999; Donovan *et al.* 2011). Using a mutant approach we show clear evidence that silencing the pleiotropic genes underlying the LES did not result in aberrant (i.e. out of the RILs pattern) or non-viable phenotypes but instead resulted in a coordinated adjustment of all physiological leaf traits. This result suggests that the LES is 'hardwired' into the genome. Specifically, due to direct pleiotropic effects or indirect physiological linkages, *CRY2* and *HUA2* constrain the space of possible trait values so as to avoid a change in one trait without a change in other correlated traits. Differences between phenotypes of NILs and mutants (such as between Cvi-FLG_{Ler} and $hua2_{Col}$) can be explained by *i*) the effect of the genetic background, *ii*) the contrasted effects of silencing one gene in KO-mutants versus carrying a natural variant of this gene in NILs, or *iii)* the effects of other genes in the introgressed regions. As suggested by the differences in the phenotypes of $cry2_{Ler}$ and Cvi-EDI_{Ler}, unknown genes, linked to *CRY2* and *HUA2* in *EDI* and *FLG* respectively, could contribute to the QTL effects. For instance, *HUA2* has been shown to be mediated by the effect of a co-locating QTL, *FLC*, that acts as a positive regulator of *HUA2* effects (Mendez-Vigo *et al.* 2010). Together these findings suggest that genetic constraints limit the range of leaf trade-offs to a spectrum of covariations, but selection on major pleiotropic genes could arise inside the spectrum for a plant to take advantage of, depending on the environment, different optimal combinations of leaf economics.

We propose that, in general, across environmental gradients selection will act on leaf economics traits to select for genotypes that maintain an approximate ¾-power scaling of growth, but yet different LES trait values and thus result in the local adaptation of populations (Mitchell-Olds & Schmitt 2006; Alonso-Blanco *et al.* 2009). This does not necessarily imply

418 that selection, in certain environments, could result in different values of the allometric
419 exponent (Price *et al.* 2007) but rather is consistent with the general argument made by both
420 LES and MST that, ultimately, botanical scaling relationships are the outcome of natural
421 selection (West *et al.* 1999b; Enquist *et al.* 2007a). If the same pleiotropic mechanism is
422 general across Embryophytes then multiple *intra*- and *inter*-specific scaling relationships at
423 the leaf and whole-plant levels could be tightly linked to genetic variability in few genes.
424
425 MST has been criticized on empirical, statistical, and theoretical grounds (e.g. Riisgard
426 1998; Glazier 2005; Reich *et al.* 2006) in part because of the difficulty in testing its basic
427 assumptions (Enquist & Bentley 2012). Our study, for the first time, tests several of the
428 fundamental evolutionary assumptions that underlie MST. Similarly, by translating the trade-
429 offs between structural investment for longevity and return on investment in carbon and
430 nitrogen, the LES has been hypothesized to be the outcome of natural selection to optimize
431 leaf carbon balance within a given environment (Reich *et al.* 1999; Blonder *et al.* 2011;
432 Donovan *et al.* 2011). Our results show that leaf economics and variation in metabolic
433 allometries, at least in Arabidopsis, are intimately linked through the effects of key genes.
434 Together, these findings support Chapin's (1993) hypothesis that variation in leaf and other
435 plant metabolic traits have a common genetic underpinning and that evolutionary filtering of a
436 small number of antagonistic pleiotropic genes could be at the origin of many botanical
437 scaling relationships.
438
439
440 **Acknowledgements:** We thank M. Dauzat, A. Bédié, F. Bouvery, C. Balsera, J. Bresson and
441 G. Rolland for technical assistance; M. Dauzat and K.J. Parkinson for designing the
442 *Arabidopsis* whole-plant gas exchange chamber for CIRAS II. We thank N. Whiteman, M.

443 Koornneef, S. Tisné, M. Reymond and B. Shipley for helpful comments, and J. Keurentjes for
444 discussions on RILs and data supply. The authors are grateful to three anonymous reviewers
445 for constructive comments and manuscript improvement. FV was funded by a CIFRE grant
446 (ANRT, French Ministry of Research) supported by BAYER Crop Science (contract
447 0398/2009 - 09 42 008). CV was supported by a Marie Curie International Outgoing
448 Fellowship within the 7th European Community Framework Program (DiversiTraits project,
449 no. 221060). BJE was supported by an NSF ATB award.
450
451

References

Alonso-Blanco C., Peeters A.J.M., Koornneef M., Lister C., Dean C., van den Bosch N. *et al.* (1998a). Development of an AFLP based linkage map of L*er*, Col and Cvi *Arabidopsis thaliana* ecotypes and construction of a L*er*/Cvi recombinant inbred line population. *Plant J.*, 14, 259-271.

Alonso-Blanco C., El-Assal S.E.D., Coupland G. & Koornneef M. (1998b). Analysis of natural allelic variation at flowering time loci in the Landsberg erecta and Cape Verde islands ecotypes of *Arabidopsis thaliana*. *Genetics*, 149, 749-764.

Alonso-Blanco C., Aarts M.G.M., Bentsink L., Keurentjes J.J.B., Reymond M., Vreugdenhil D. *et al.* (2009). What has natural variation taught us about plant development, physiology, and adaptation? *Plant Cell*, 21, 1877-1896.

Baraloto C., Paine C.E.T., Poorter L., Beauchene J., Bonal D., Domenach A.M. *et al.* (2010). Decoupled leaf and stem economics in rain forest trees. *Ecol. Lett.*, 13, 1338-1347.

Blonder B., Violle C., Bentley L.P. & Enquist B.J. (2011). Venation networks and the origin of the leaf economics spectrum. *Ecol. Lett.*, 14, 91-100.

Bomblies K., Lempe J., Epple P., Warthmann N., Lanz C., Dangl J.L. *et al.* (2007). Autoimmune response as a mechanism for a Dobzhansky-Muller-type incompatibility syndrome in plants. *Plos Biol.*, 5, 1962-1972.

Chapin F.S., Autumn K. & Pugnaire F. (1993). Evolution of suites of traits in response to environmental stress. *Am. Nat.*, 142, S78-S92.

Charnov E.L. (1993). *Life history invariants : some explorations of symmetry in evolutionary ecology*. Oxford University Press, Oxford England ; New York.

Coleman J.S., McConnaughay K.D.M. & Ackerly D.D. (1994). Interpreting phenotypic variation in plants. *Trends Ecol. Evol.*, 9, 187-191.

Donovan L.A., Maherali H., Caruso C.M., Huber H. & de Kroon H. (2011). The evolution of the worldwide leaf economics spectrum. *Trends Ecol. Evol.*, 26, 88-95.

Doyle M.R., Bizzell C.M., Keller M.R., Michaels S.D., Song J.D., Noh Y.S. *et al.* (2005). HUA2 is required for the expression of floral repressors in *Arabidopsis thaliana*. *Plant J.*, 41, 376-385.

Edwards C.E., Ewers B.E., Williams D.G., Xie Q.G., Lou P., Xu X.D. *et al.* (2011). The genetic architecture of ecophysiological and circadian traits in *Brassica rapa*. *Genetics*, 189, 375-U1107.

El-Assal S.E.D., Alonso-Blanco C., Peeters A.J.M., Raz V. & Koornneef M. (2001). A QTL for flowering time in *Arabidopsis* reveals a novel allele of *CRY2*. *Nat. Genet.*, 29, 435-440.

Enquist B.J., Tiffney B.H. & Niklas K.J. (2007a). Metabolic scaling and the evolutionary dynamics of plant size, form, and diversity: Toward a synthesis of ecology, evolution, and paleontology. *Int. J. Plant Sci.*, 168, 729-749.

Enquist B.J., Allen A.P., Brown J.H., Gillooly J.F., Kerkhoff A.J., Niklas K.J. *et al.* (2007b). Does the exception prove the rule? *Nature*, 445, E9-E10.

Enquist B.J. & Bentley L.P. (2012). Land plants: new theoretical directions and empirical prospects. In: *Metabolic ecology: a scaling approach* (eds. Sibly RM, Brown JH & Kodric-Brown A). John Wiley & Sons Chichester, pp. 164-187.

Flood P.J., Harbinson J. & Aarts M.G. (2011). Natural genetic variation in plant photosynthesis. *Trends in Plant Sci.*, 16, 327-35.

Fu J., Keurentjes J.J., Bouwmeester H., America T., Verstappen F.W., Ward J.L. *et al.* (2009). System-wide molecular evidence for phenotypic buffering in Arabidopsis. *Nat. Genet.*, 41, 166-7.

501 Givnish T.J. (1988). Adaptation to sun and shade - a whole-plant perspective. *Aust. J. Plant*
502 *Physiol.*, 15, 63-92.
503 Glazier D.S. (2005). Beyond the '3/4-power law': variation in the intra- and interspecific
504 scaling of metabolic rate in animals. *Biol. Rev.*, 80, 611-662.
505 Gould S.J. (1966). Allometry and size in ontogeny and phylogeny. *Biol. Rev.*, 41, 587-640.
506 Granier C., Aguirrezabal L., Chenu K., Cookson S.J., Dauzat M., Hamard P. *et al.* (2006).
507 PHENOPSIS, an automated platform for reproducible phenotyping of plant responses
508 to soil water deficit in *Arabidopsis thaliana* permitted the identification of an
509 accession with low sensitivity to soil water deficit. *New Phytol.*, 169, 623-35.
510 Hancock A.M., Brachi B., Faure N., Horton M.W., Jarymowycz L.B., Sperone F.G. *et al.*
511 (2011). Adaptation to climate across the *Arabidopsis thaliana* genome. *Science*, 334,
512 83-6.
513 Huxley J.S. (1932). *Problems of relative growth*. Methuen & co. LTD, London.
514 Keurentjes J.J., Bentsink L., Alonso-Blanco C., Hanhart C.J., Blankestijn-De Vries H., Effgen
515 S. *et al.* (2007). Development of a near-isogenic line population of *Arabidopsis*
516 *thaliana* and comparison of mapping power with a recombinant inbred line population.
517 *Genetics*, 175, 891-905.
518 Kikuzawa K. (1991). A cost-benefit-analysis of leaf habit and leaf longevity of trees and their
519 geographical pattern. *Am. Nat.*, 138, 1250-1263.
520 Kikuzawa K. & Lechowicz M.J. (2006). Toward synthesis of relationships among leaf
521 longevity, instantaneous photosynthetic rate, lifetime leaf carbon gain, and the gross
522 primary production of forests. *Am. Nat.*, 168, 373-383.
523 Kolokotrones T., Savage V., Deeds E.J. & Fontana W. (2010). Curvature in metabolic scaling.
524 *Nature*, 464, 753-756.

525 Masle J., Gilmore S.R. & Farquhar G.D. (2005). The *ERECTA* gene regulates plant
526 transpiration efficiency in Arabidopsis. *Nature*, 436, 866-70.
527 McKay J.K., Richards J.H. & Mitchell-Olds T. (2003). Genetics of drought adaptation in
528 *Arabidopsis thaliana*: I. Pleiotropy contributes to genetic correlations among
529 ecological traits. *Mol. Ecol.*, 12, 1137-1151.
530 Mendez-Vigo B., Andres M., Ramiro M., Martinez-Zapater J.M. & Alonso-Blanco C. (2010).
531 Temporal analysis of natural variation for the rate of leaf production and its
532 relationship with flowering initiation in *Arabidopsis thaliana*. *J. Exp. Bot.*, 1611-1623.
533 Metcalf C.J.E. & Mitchell-Olds T. (2009). Life history in a model system: opening the black
534 box with *Arabidopsis thaliana*. *Ecol. Lett.*, 12, 593-600.
535 Mitchell-Olds T. & Schmitt J. (2006). Genetic mechanisms and evolutionary significance of
536 natural variation in *Arabidopsis*. *Nature*, 441, 947-952.
537 Mori S., Yamaji K., Ishida A., Prokushkin S.G., Masyagina O.V., Hagihara A. *et al.* (2010).
538 Mixed-power scaling of whole-plant respiration from seedlings to giant trees. *Proc.*
539 *Natl. Acad. Sci. USA*, 107, 1447-1451.
540 Niklas K.J. (1994). *Plant allometry - The scalling of form and process*. First edn. The
541 University of Chicago Press, Chicago.
542 Olson M.E., Aguirre-Hernandez R. & Rosell J.A. (2009). Universal foliage-stem scaling
543 across environments and species in dicot trees: plasticity, biomechanics and Corner's
544 Rules. *Ecol. Lett.*, 12, 210-219.
545 Pavlicev M. & Wagner G.P. (2012). A model of developmental evolution: selection,
546 pleiotropy and compensation. *Trends Ecol. Evol.*, 27, 316-322.
547 Poorter H., van Rijn C.P.E., Vanhala T.K., Verhoeven K.J.F., de Jong Y.E.M., Stam P. *et al.*
548 (2005). A genetic analysis of relative growth rate and underlying components in
549 *Hordeum spontaneum*. *Oecologia*, 142, 360-377.

550 Price C.A., Enquist B.J. & Savage V.M. (2007). A general model for allometric covariation in
551 botanical form and function. *Proc. Natl. Acad. Sci. USA*, 104, 13204-9.
552 Reich P.B., Walters M.B. & Ellsworth D.S. (1997). From tropics to tundra: Global
553 convergence in plant functioning. *Proc. Natl. Acad. Sci. USA*, 94, 13730-13734.
554 Reich P.B., Ellsworth D.S., Walters M.B., Vose J.M., Gresham C., Vollin J.C. *et al.* (1999).
555 Generality of leaf trait relationships : A test across six biomes. *Ecology*, 80, 1955-
556 1969.
557 Reich P.B., Tjoelker M.G., Machado J.L. & Oleksyn J. (2006). Universal scaling of
558 respiratory metabolism, size and nitrogen in plants. *Nature*, 439, 457-461.
559 Riisgard H.U. (1998). No foundation of a "3/4 power scaling law" for respiration in biology.
560 *Ecol. Lett.*, 1, 71-73.
561 Shipley B., Lechowicz M.J., Wright I. & Reich P.B. (2006). Fundamental trade-offs
562 generating the worldwide leaf economics spectrum. *Ecology*, 87, 535-541.
563 Tisné S., Reymond M., Vile D., Fabre J., Dauzat M., Koornneef M. *et al.* (2008). Combined
564 genetic and modeling approaches reveal that epidermal cell area and number in leaves
565 are controlled by leaf and plant developmental processes in *Arabidopsis*. *Plant*
566 *Physiol.*, 148, 1117-1127.
567 Wang Q., Sajja U., Rosloski S., Humphrey T., Kim M.C., Bomblies K. *et al.* (2007). *HUA2*
568 caused natural variation in shoot morphology of *A. thaliana*. *Curr. Biol.*, 17, 1513-
569 1519.
570 West G.B., Brown J.H. & Enquist B.J. (1999a). A general model for the structure and
571 allometry of plant vascular systems. *Nature*, 400, 664-667.
572 West G.B., Brown J.H. & Enquist B.J. (1999b). The fourth dimension of life: fractal geometry
573 and allometric scaling of organisms. *Science*, 284, 1677-1679.

574 Westoby M., Warton D. & Reich P.B. (2000). The time value of leaf area. *Am. Nat.*, 155, 649-
575 656.
576 Westoby M., Falster D.S., Moles A.T., Vesk P.A. & Wright I.J. (2002). Plant ecological
577 strategies: Some leading dimensions of variation between species. *Annu. Rev. Ecol.*
578 *Syst.*, 33, 125-159.
579 Wright I.J., Reich P.B., Westoby M., Ackerly D.D., Baruch Z., Bongers F. *et al.* (2004). The
580 worldwide leaf economics spectrum. *Nature*, 428, 821-827.
581
582
583 **SUPPORTING INFORMATION**
584 Additional Supporting Information may be downloaded via the online version of this article at
585 Wiley Online Library (www.ecologyletters.com).
586

587 **Table 1. Correlations between traits, heritabilities and percentage of variation explained**
588 **by the loci *EDI* and *FLG* in the recombinant inbred lines.** Pearson's correlations (lower
589 matrix). Broad-sense heritabilities (H^2). Plant dry mass (M); allometric exponent (θ_q); leaf dry
590 mass per area (LMA). No epistatic interactions were found between *EDI* and *FLG* (P > 0.05)
591 except for N concentration (see Supporting Information). Data from Experiment 1.
592

	M	Growth rate	θ_q	Age at flowering	Photosynthetic rate	LMA	H^2 (%)	EDI (%)	FLG (%)
M							0.89	23.8	21.4
Growth rate	0.98						0.84	25.8	19.5
θ_q	-0.98	-0.96					0.90	33.8	21.9
Age at flowering	0.96	0.91	-0.97				0.82	26.8	23.1
Photosynthetic rate	-0.92	-0.86	0.94	-0.95			0.80	29.3	19.1
LMA	0.94	0.93	-0.94	0.93	-0.93		0.68	25.2	21.3
N concentration	-0.60	-0.53	0.66	-0.67	0.72	-0.66	-	19.1	16.4

593
594

595 **Figure legends**

596

597 **Figure 1. Variation of physiological and growth-related traits in the *A. thaliana* L*er* ×**

598 **Cvi RIL population.** (**A**) plant dry mass (*M*); (**B**), growth rate; (**C**), mass-based

599 photosynthetic rate; (**D**), N concentration; (**E**) age at flowering and (**F**) leaf dry mass per area

600 (LMA). Bars are means ± *se* for each RIL (n = 4 except for N concentration n = 1) and for the

601 parents (L*er* and Cvi; arrows; n = 8 except for N concentration n = 1). Data from Experiment

602 1. Lines ordered by increasing plant dry mass.

603

604 **Figure 2. *EDI* and *FLG* effects on the allometric scaling of plant growth.** (**A**) Regression

605 lines and equations (standardized major axis) of the relationships between aboveground plant

606 dry mass (*M*) and growth rate shown across individuals for the four sub-populations defined

607 by the two loci *EDI* and *FLG*. Parental types Cvi/Cvi (yellow squares) and L*er*/L*er* (green

608 circles), and recombinant types Cvi/L*er* (blue upward triangles) and L*er*/Cvi (red downward

609 triangles) at the two loci *EDI*/*FLG*, respectively. (**B**) Density distributions and box-and-

610 whisker plots of the local allometric exponent θ_q according to the allelic combination at the

611 two QTLs (same colors used). Vertical dotted line: expected θ value (0.75) of allometric

612 exponent following MST predictions. Asterisks represent significant differences from 0.75 (P

613 < 0.001). Data from Experiment 1.

614

615 **Figure 3. QTL analysis of the allometric exponent of plant growth and of the traits**

616 **underlying the leaf economics.** Likehood value of a QTL presence at the specified position

617 along the five chromosomes (LOD score) for (**A**) the allometric exponent of plant growth (θ_q),

618 and (**B**) the traits underlying the leaf economics. LMA: leaf dry mass per area. Dotted lines:

619 maximum significance threshold across traits (2.9). Data from Experiment 1.

Figure 4. ***EDI* and *FLG* effects on the patterns of correlation between the traits underlying the leaf economics in the *A. thaliana* L*er* × Cvi RIL population.** Each point is the mean value of four replicates per RIL (except for N concentration, $n = 1$). Parental types Cvi/Cvi (yellow squares) and L*er*/L*er* (green circles), and recombinant types Cvi/L*er* (blue upward triangles) and L*er*/Cvi (red downward triangles) at the two loci *EDI*/*FLG*, respectively. LMA: leaf dry mass per area. Bivariate relationships are shown on 2D plans (grey dotted symbols). See Table 1 for correlation statistics. Data from Experiment 1.

Figure 5. **QTL confirmation and validation of *CRY2* and *HUA2* as major contributors of the variation in leaf economics and scaling allometry of plant growth in Arabidopsis.** Projections of mean ± sd (n = 3-10) trait values of NILs, KO-mutants and wild-types (Experiment 2) in the patterns of leaf economics (**A-E**) and allometric scaling relationships (**F**) observed across RILs (Experiment 1, grey points). NILs are Cvi fragments introgressed into L*er* at the top of chromosome I (Cvi-EDI_{Ler}; red plus sign) and in the middle of chromosome V (Cvi-FLG_{Ler}; red cross). $cry2_{Ler}$ (red circle) and $cry2_{Col}$ (blue point up triangle) are KO-mutants of *CRY2* in L*er* (red filled circle) and Col (blue filled triangle) genetic backgrounds, respectively. $hua2_{Col}$ (blue point down triangle) is a KO-mutant of *HUA2* in Col background. Cvi (red point up triangle). Leaf dry mass per area (LMA); plant dry mass (M).

Figure 1.

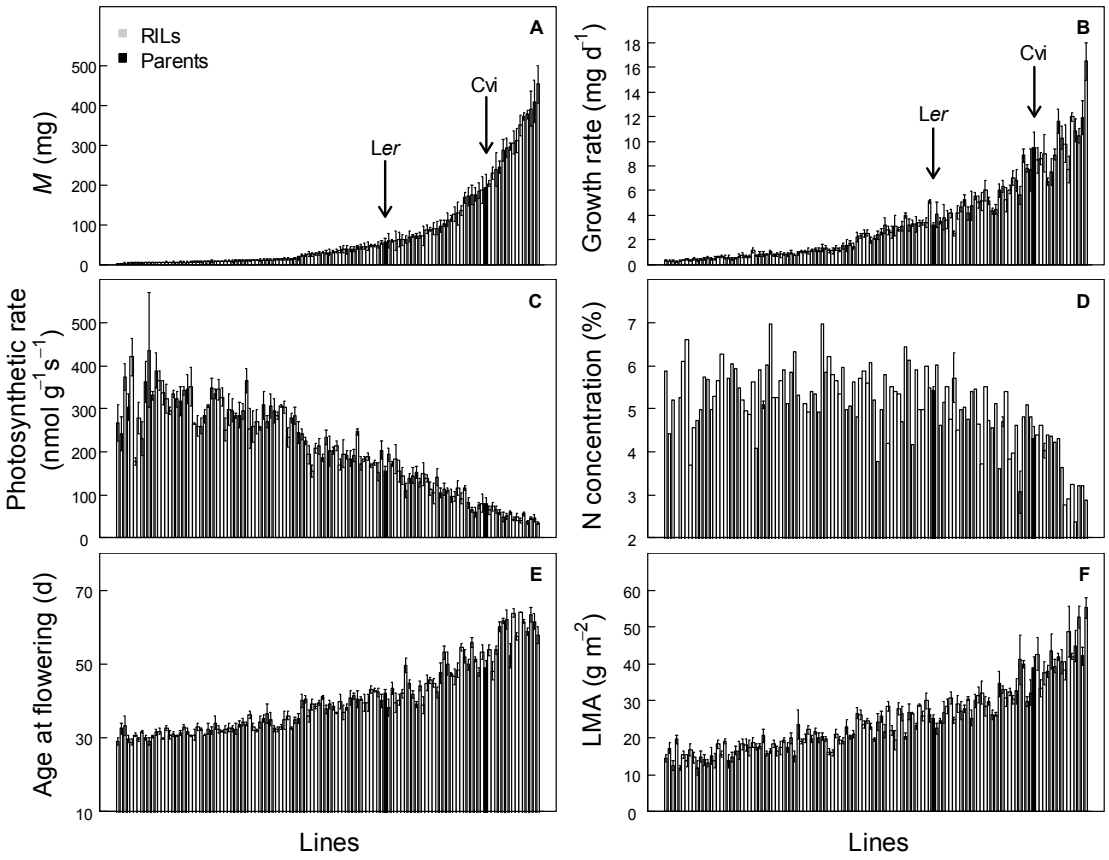
RILs
Parents
A
B
C
D
E
F
M (mg)
Growth rate (mg d^{-1})
Photosynthetic rate (nmol g^{-1}s^{-1})
N concentration (%)
Age at flowering (d)
LMA (g m^{-2})
Ler
Cvi
Lines
Lines

Figure 2.

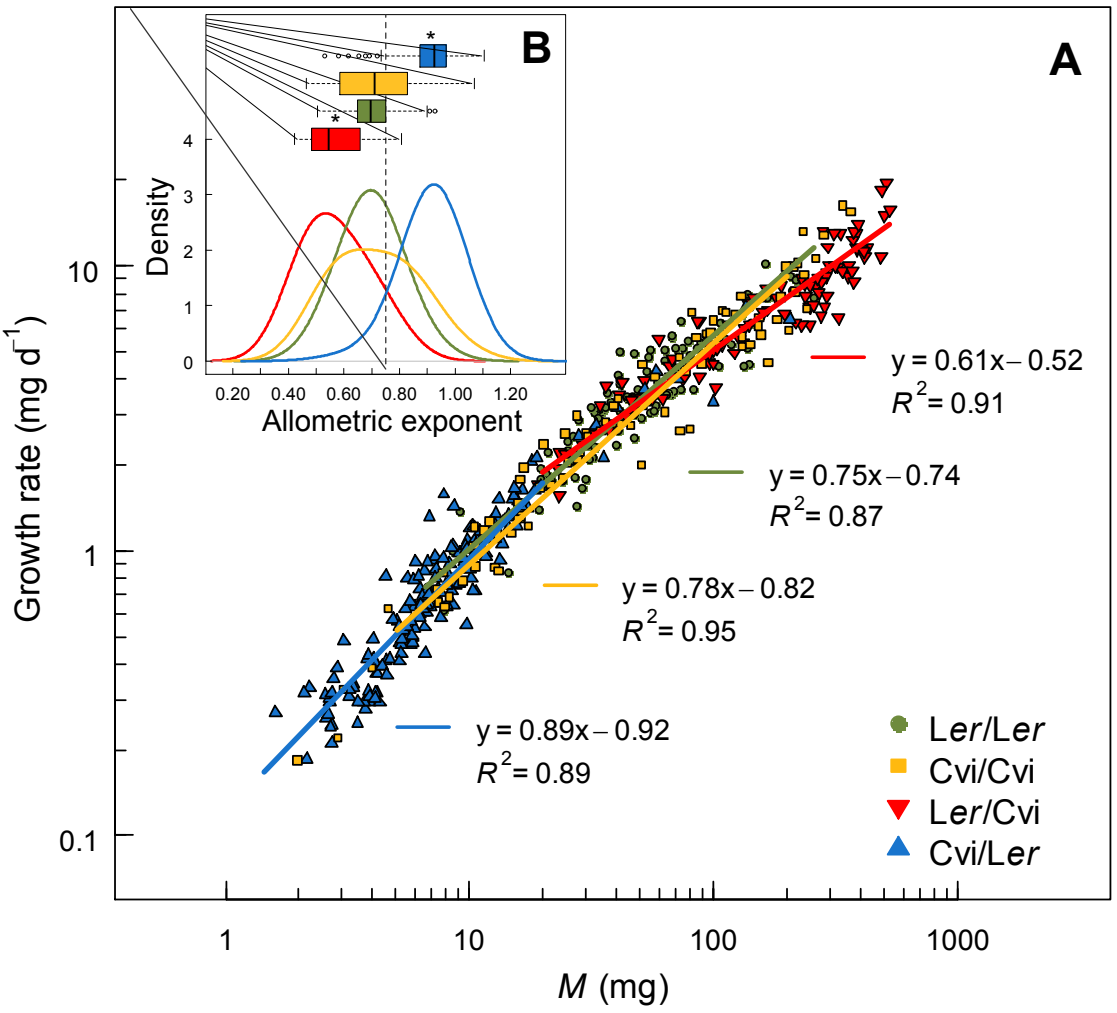
A
B
Growth rate (mg d^{-1})
M (mg)
1
10
100
1000
0.1
1
10
Density
0
1
2
3
4
0.20
0.40
0.60
0.80
1.00
1.20
Allometric exponent
y = 0.61x – 0.52
R^2 = 0.91
y = 0.75x – 0.74
R^2 = 0.87
y = 0.78x – 0.82
R^2 = 0.95
y = 0.89x – 0.92
R^2 = 0.89
Ler/Ler
Cvi/Cvi
Ler/Cvi
Cvi/Ler

Figure 3.

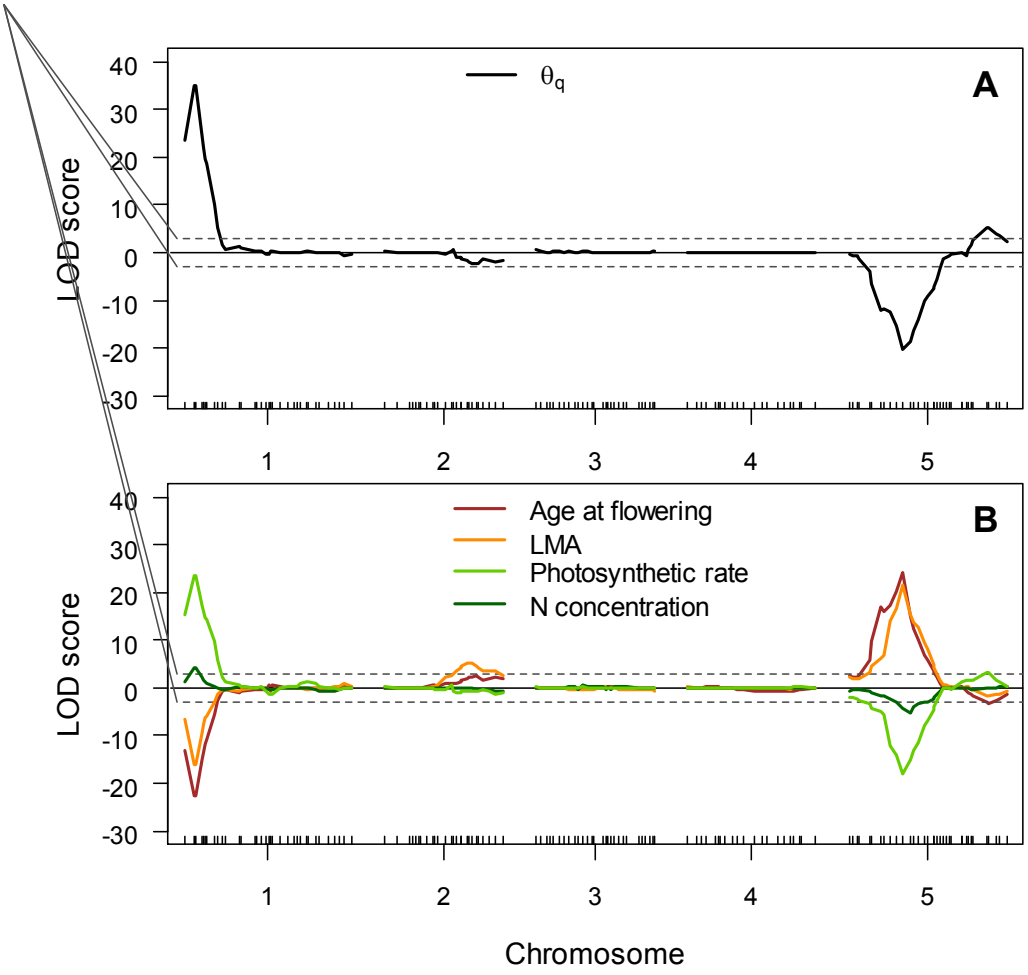
A
θ_q
LOD score
40
30
20
10
0
-10
-20
-30
1
2
3
4
5
B
Age at flowering
LMA
Photosynthetic rate
N concentration
LOD score
Chromosome

Figure 4.

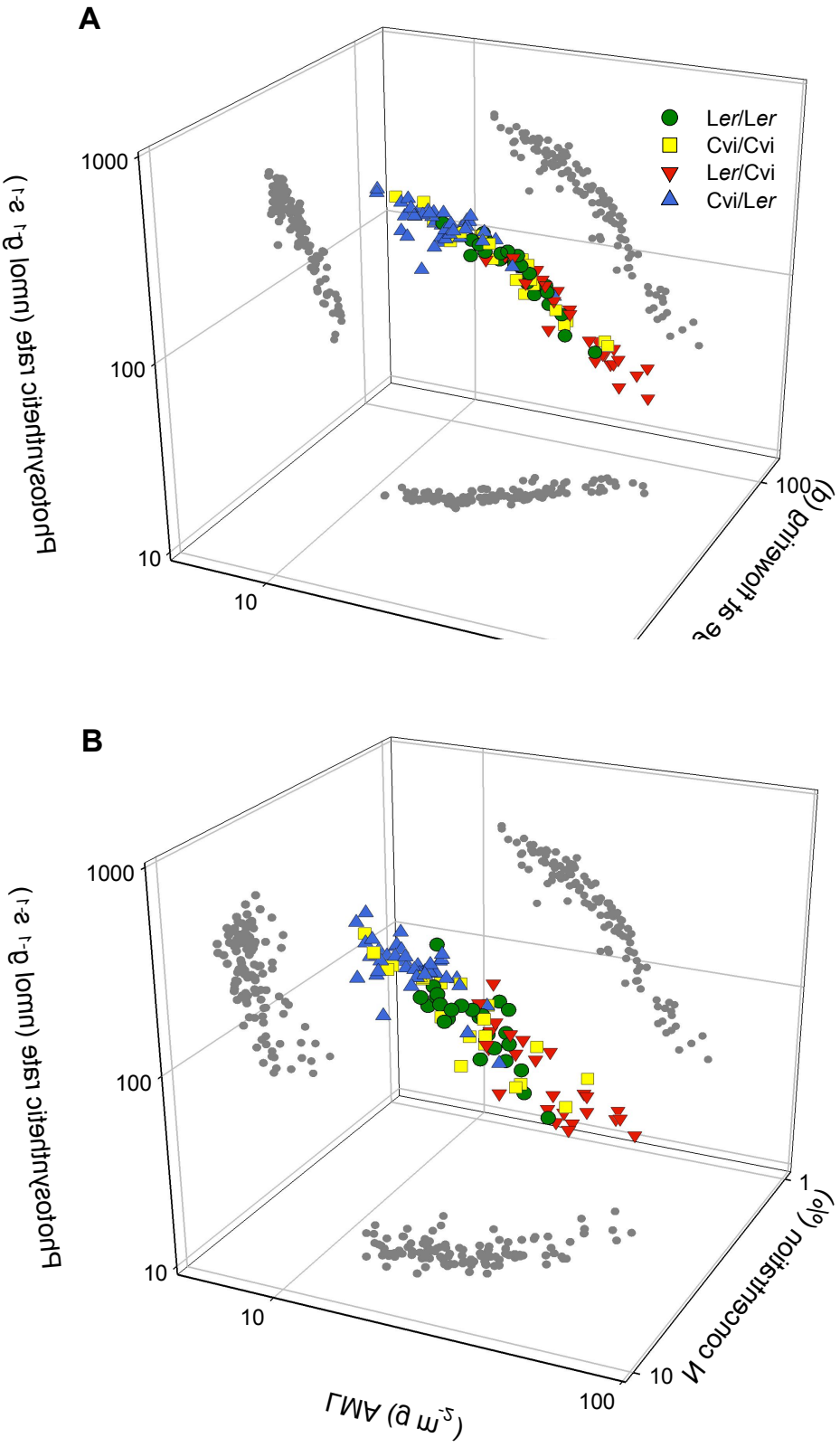
A
Ler/Ler
Cvi/Cvi
Ler/Cvi
Cvi/Ler
1000
100
10
10
100
B
1000
100
10
10
100
10
1
Photosynthetic rate (μmol g-1 s-1)
LMA (g m-2)
N concentration (%)

Figure 5.

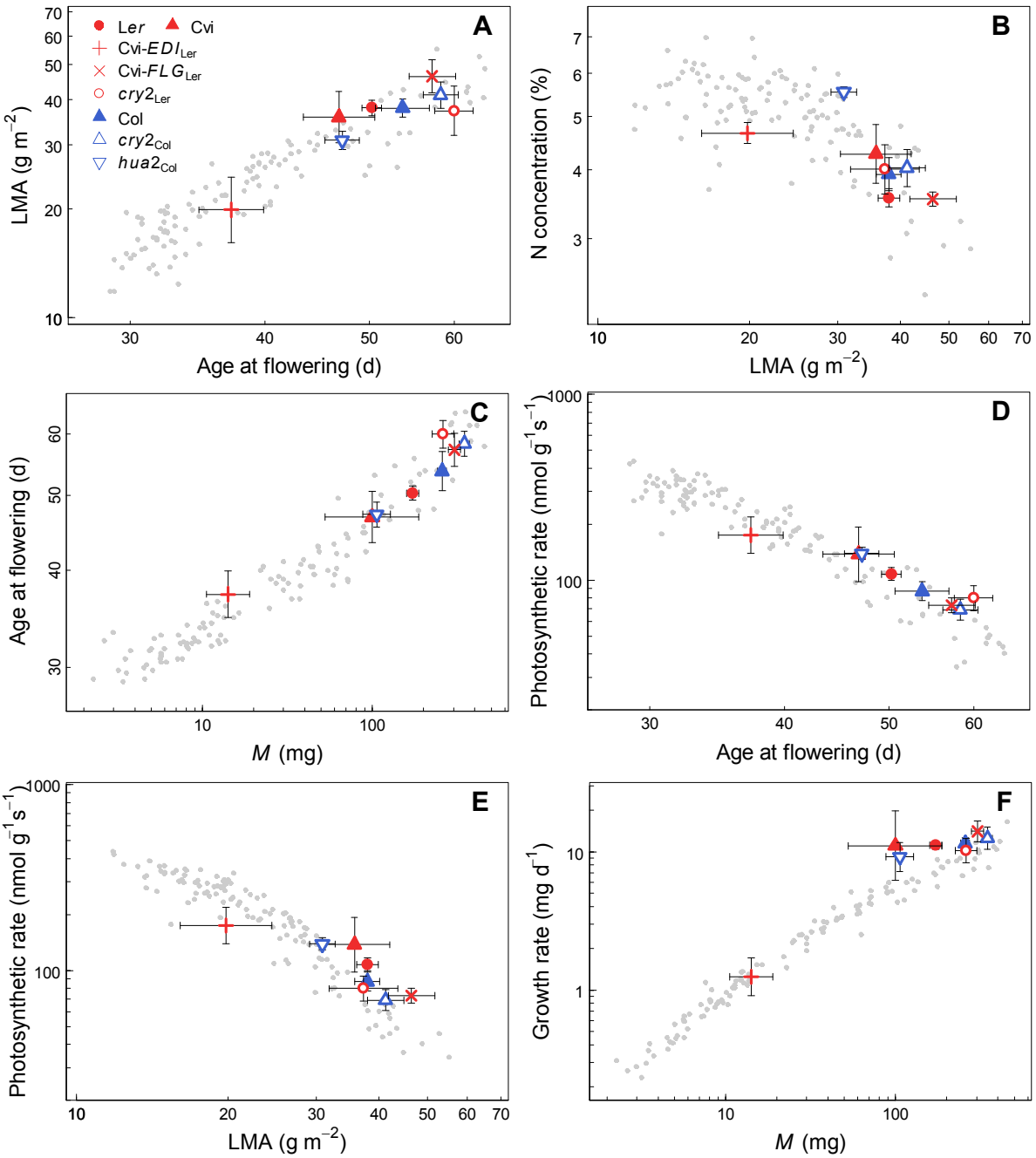
A
Ler
Cvi
Cvi-EDI Ler
Cvi-FLG Ler
cry2 Ler
Col
cry2 Col
hua2 Col
LMA (g m−2)
Age at flowering (d)
B
N concentration (%)
LMA (g m−2)
C
Age at flowering (d)
M (mg)
D
Photosynthetic rate (nmol g−1 s−1)
Age at flowering (d)
E
Photosynthetic rate (nmol g−1 s−1)
LMA (g m−2)
F
Growth rate (mg d−1)
M (mg)